Chapter 16
Joint Electricity and Heat Optimal Power Flow of Energy Hubs

Manijeh Alipour, Kazem Zare, and Heresh Seyedi

16.1 Introduction

Electricity is the utmost popular type of energy in recent days. All developed sectors of countries almost utilize electrical energy. In addition to the electricity, there are heating and cooling demands that should be supplied. Therefore, another transmission network, district heating network (DHN), is the other important system, which is very promising for carbon emission reduction and energy saving. District heating network is a well-extended system in several Northern European countries [1]. Conventionally, most energy service networks, i.e., electricity and local district heating systems have been scheduled separately without considering interdependency between various energy service infrastructures. Nevertheless, many welfares can be attained by envisaging the energy service system as cohesive. Energy flows provided from alternative resources could be administrated and consequently, safety of energy preparation can be improved. The energy could be supplied more efficiently and energy emissions, losses and costs would be reduced. However, in the case of separate planning and operation of energy systems an unlikely optimal solution will be reached, since optimization of each transmission network separately can obscure the optimal operation of the entire energy system. Henceforth, a unified study of energy networks is highly desirable [2, 3] and recent studies suggest integration of these networks so-called multi-carrier energy networks (MCENs) [2, 4, 5]. The important motivation behind aforesaid viewpoint is the growing exploitation of co-generation systems which creates a potent connection among various networks [2].

M. Alipour · K. Zare · H. Seyedi (✉)
Faculty of Electrical and Computer Engineering, University of Tabriz, Tabriz, Iran
e-mail: alipour@tabrizu.ac.ir; kazem.zare@tabrizu.ac.ir; hseyedi@tabrizu.ac.ir

The interdependency of these industries necessitates the integrated optimization of joint energy networks. For instance, a combined heat and power (CHP) unit generates electricity and heat by employing natural gas [6]. It connects the electrical network to the district heating and natural gas networks. Hence, these networks should be taken into account together as an integrated system for an optimization procedure that forms the so-called MCEN. The concept energy hub opens a new window on demonstration of a unified energy network which comprises several energy carriers such as heat, electricity, gas, etc. The concept of energy hub was first introduced in [7]. It can be specified as a mixture of energy conversion units which meets various kinds of energy demands [8]. Currently, multi-generation systems called as energy hub for combined and distributed generation of various energy sources can be established owing to advances in energy substructures. Energy hub can be envisioned as an integrated system where numerous energy carriers are stored, converted, and distributed [9, 10]. Compliance of multi-generation systems conveys noteworthy benefits in terms of improved energy efficiency, enhanced economy, and reduced CO2 emissions [11, 12]. The integration of several energy networks is investigated in some works [2, 4, 13]. These methodologies utilize energy hub model for the energy system. A heuristic optimization scheme is developed in [14] for multi-carrier systems.

Nowadays, the hubs are subject to more instable electricity prices as a result of liberalized electricity markets and are enthusiastic to alter their consumption pattern in order to diminish the costs. Demand response program (DRP) is one of the prevailing techniques of demand side management in which electricity end-users adapt their demand profile in response to operators request and/or electricity prices [15, 16]. The DRP is modeled and employed in various papers to evaluate the impact of DRP on electric demand profile characteristics [17, 18]. In Wu et al. [17], DRP is integrated in the scheduling model in order to manage the volatility of renewable energy. A new DRP has been proposed in [18] for distribution feeders with smart loads. An energy hub model in which distributed generations and electric load DRP are modeled and incorporated to gas and electricity substructures has been studied in [19]. Moreover, the DRP is formulated for the natural gas and electricity networks in [20]. The total daily heating and electricity demands of hub are supplied in [20].

On the other hand, the heating load profile of the MCEN can be modified in order to handle the interdependency of heat and power in CHP units and take more advantages of the units in producing power and heat with high efficiency. The thermal loads of a typical MCEN are responsive and flexible due to two motives. First, the human easement region is not a point but a span [21]. Second, warming can benefit present as well as adjoining future hours, since thermic insulation causes the thermal energy to be stocked. Therefore, regarding the proposed demand response program, in contrast to existing papers, the MCEN takes advantages of the curtailable and responsive heating demand of DHN. In addition, the hubs' thermal load will be modified regarding electric load profile in order to derive advantage of CHP units and alleviate total cost of provision of energy.

16.2 Basic Concepts of Multi-Carrier Energy Systems

This section introduces the energy hub concept and MCEN substructures model since the MCENs' prosperous role in future perspective of energy systems will precisely be distinguished through their basic components.

16.2.1 Energy Hub

Energy hub encompasses various technologies and devices. Firstly a typical energy hub model is described to clarify the optimization problem process. A generic energy hub model is presented in Fig. 16.1. As it is clear, the input energy carriers of hub are natural gas and electricity and the output side consists of thermal and electrical energies which will supply the heat and electric demands. The system converters are composed of a transformer, a micro-turbine, and a gas furnace. The input gas is dispersed between the micro-turbine and gas furnace. The micro-turbine uses natural gas and generates heat and electricity. In addition, the gas furnace generates heat from input natural gas.

The energy hub gets the information from day-ahead market and the hub's input and output states are liable for establishing optimal operation based on collected data. It is worth bearing in mind that the considered market in this chapter is a perfect
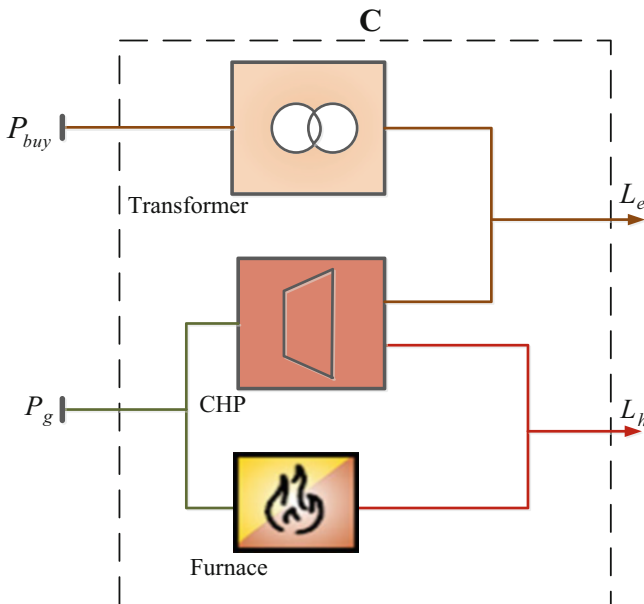

Fig. 16.1 Representation of a typical energy hub

market where all players are price takers. Therefore, the multi-carrier energy system only employs the market prices for optimal scheduling of hub and its strategies cannot affect the market price.

16.2.2 Multi-Carrier Energy System Structure

The carriers of the multi-carrier energy system are transferred to hubs via various transmission networks. The heat and electricity networks are typically connected through the coupling facilities of hubs (e.g., circulation pumps and CHP units). These coupling facilities permit the streams of energy among the networks. CHP units produce heat and power simultaneously; circulation pumps use electrical energy to circulate the water in the DHN. These hubs' converters enhance the flexibility of the heat and electricity systems for assisting the incorporation of uncertain renewable energy [22].

16.3 Problem Formulation

Integrated optimal thermal and electrical power flow constrained scheduling model of MCEN considering heat demand response is presented in this chapter. The aim of the optimal operational scheduling is minimizing the overall cost of hubs' power and heat procurement over a day-ahead period of time, satisfying several constraints.

16.3.1 Objective Function

The purpose of the MCEN scheduling is minimizing the cost of meeting hubs demands. The objective function in the thermal and electrical power flow constrained scheduling problem of MCEN to be minimized encompasses the expense of purchased power and gas from the main grid. Moreover, the MCEN is supposed to be capable of selling power to the main grid. Then, maximizing the income from selling the additional power to the grid is integrated in the objective function. The objective function to be optimized is as follows:

$$\underset{Pg_{h,t}, P_t^{\text{grid}}}{\text{minimize}} \sum_t \left\{ P_t^{\text{grid}} \gamma_{e,t} + \sum_h Pg_{h,t} \gamma_{g,t} \right\} + H_{\text{Cur}} \gamma_{\text{Cur}} \qquad (16.1)$$

It should be mentioned that, the interchanged power with the main grid, P_t^{grid}, would be positive in the case of buying power from the grid, else it would be negative. $H_{\text{Cur}} \gamma_{\text{Cur}}$ is the cost of curtailed load. In order to model the technical

constraints related to various energy networks, the mathematical representations of district heat and electricity networks power flow will be addressed in the following.

16.3.2   Analysis of District Heating Networks

Heat can be produced at hubs by heat sources like CHPs or furnaces, and conveyed by water in supply pipe network. The water temperature drops at consumers' sites, owing to the heat consumption and supplies back to the hub through a return pipeline. Key DHS elements comprising heat sources, heat-exchangers, and the network of pipelines are modeled in Sects. 16.3.2.1–16.3.2.6.

16.3.2.1   Heat Sources

In general, heat sources include CHP units and gas furnaces that supply heat. CHP units and gas furnaces are modeled in the following:

$$Pg_{h,t} = Pg_{h,t}^{\text{CHP}} + Pg_{h,t}^{F} \tag{16.2}$$

$$H_{h,t}^{F} = \eta^{F} Pg_{h,t}^{F} \tag{16.3}$$

$$H_{h,t}^{\text{CHP}} = \eta_{q}^{\text{CHP}} Pg_{h,t}^{\text{CHP}} \tag{16.4}$$

$$P_{h,t}^{\text{CHP}} = \eta_{e}^{\text{CHP}} Pg_{h,t}^{\text{CHP}} \tag{16.5}$$

$$H_{h,t}^{\text{HS}} = H_{h,t}^{\text{CHP}} + H_{h,t}^{F} \tag{16.6}$$

$$\underline{H}^{F} \leq H_{h,t}^{F} \leq \overline{H}^{F} \tag{16.7}$$

$$\underline{H}^{\text{CHP}} \leq H_{h,t}^{\text{CHP}} \leq \overline{H}^{\text{CHP}} \tag{16.8}$$

Referring to (16.2), the purchased gas, $Pg_{h,t}$, is distributed between two streams. The $Pg_{h,t}^{\text{CHP}}$ is fed into the CHP unit and the $Pg_{h,t}^{F}$ is fed into the gas furnace. Total heat output of hub h ($H_{h,t}^{\text{HS}}$) is produced using furnace and CHP units as expressed in (16.6), where η_{h}^{CHP} and η^{F} are heat efficiency of CHP unit and efficiency of furnace unit, respectively. The capacity restrictions of gas furnace and CHP unit can be described as given in (16.7) and (16.8), respectively.

16.3.2.2 Water Pumps

The pumping power, which affords the required energy to sustain the water flow in the pipelines at the hub, is proportionate to the pressure difference and mass flow rate:

$$P_{h,t}^{\text{pump}} = \frac{\dot{m}_{h,t}^{\text{HS}} \left(pr_{n,t}^{S} - pr_{n,t}^{R} \right)}{\eta_{h}^{\text{pump}} \cdot \rho} \tag{16.9}$$

where ρ and η_{h}^{pump} are water density and the efficiency of pump. The pumping power is restricted by its technical limits

$$\underline{P}_{h}^{\text{pump}} \leq P_{h,t}^{\text{pump}} \leq \overline{P}_{h}^{\text{pump}} \tag{16.10}$$

16.3.2.3 Heat Production

The constraint defining the heat output of a hub which is employed to heat the flow is:

$$H_{h,t} = c\dot{m}_{h,t} \cdot \left(T_{n,t}^{S} - T_{n,t}^{R} \right) \tag{16.11}$$

where c is specific heat. As for the supply temperature of the heat sources, there are lower and upper limits, stated as:

$$\underline{T}_{n}^{S} \leq T_{n,t}^{S} \leq \overline{T}_{n}^{S} \tag{16.12}$$

16.3.2.4 Heat-Exchange Station

Thermal energy of heat-exchangers can be modeled as follows:

$$H_{t}^{\text{HES}} = c \cdot \dot{m}_{t}^{\text{HES}} \left(T_{n,t}^{S} - T_{n,t}^{R} \right) \tag{16.13}$$

The heat exchanger pressure should be above a firm level to make sure the sustainability of mass flow:

$$pr_{n,t}^{S} - pr_{n,t}^{R} \geq \underline{pr}^{\text{HES}} \tag{16.14}$$

The return temperature of the heat exchanger should be within its lower and upper bounds as well:

$$\underline{T}_{n}^{R} \leq T_{n,t}^{R} \leq \overline{T}_{n}^{R} \tag{16.15}$$

16.3.2.5 DHN Constraints

The DHN constraints including continuity of mass flow, node temperature, heat losses from a pipe, etc., are offered in this section:

Continuity of Mass Flow

The overall mass flow rate into any DHN node would be zero:

$$\sum \dot{m} = 0 \tag{16.16}$$

Node Temperature

The combination temperature at a node is equivalent to the temperature at the start of each pipeline leaving that node [23]:

$$\sum_{l_n^-=1}^{N_1} \left(T_{l_n^-,t}^{S,\text{out}} \cdot \dot{m}_{l_n^-,t}^{S,\text{pipe}} \right) = T_{l_n^+,t}^{S,\text{in}} \cdot \sum_{l_n^-=1}^{N_l} \dot{m}_{l_n^-,t}^{S,\text{pipe}} \tag{16.17}$$

$$\sum_{l_n^+=1}^{N_1} \left(T_{l_n^+,t}^{R,\text{out}} \cdot \dot{m}_{l_n^+,t}^{R,\text{pipe}} \right) = T_{l_n^-,t}^{R,\text{in}} \cdot \sum_{l_n^+=1}^{N_l} \dot{m}_{l_n^+,t}^{R,\text{pipe}} \tag{16.18}$$

Moreover, the temperatures of mixed mass at a DHN node are equivalent to mass flowing from that node:

$$T_{l_n^+,t}^{S,\text{in}} = T_{n,t}^{S} \tag{16.19}$$

$$T_{l_n^-,t}^{R,\text{in}} = T_{n,t}^{R} \tag{16.20}$$

Heat Losses from a Pipe

The temperature reduces exponentially during water flow in the pipe [24].

$$T_{l,t}^{S,\text{out}} = T_t^a + \left(T_{l,t}^{S,\text{in}} - T_t^a \right) \cdot e^{-\frac{\lambda_l \cdot L}{c \cdot \dot{m}_{l,t}^{S,\text{pipe}}}} \tag{16.21}$$

$$T_{l,t}^{R,\text{out}} = T_t^a + \left(T_{l,t}^{R,\text{in}} - T_t^a \right) \cdot e^{-\frac{\lambda_l \cdot sL}{c \cdot \dot{m}_{l,t}^{R,\text{pipe}}}} \tag{16.22}$$

where $T_{l,t}^{S,\text{out}}$, $T_{l,t}^{R,\text{out}}$, and T_t^a are the outlet supply, outlet return, and inlet temperatures of a pipe, respectively, λ_l is heat transfer coefficient unit length, and L and $\dot{m}_{l,t}^{\text{pipe}}$ are the length and the water flow rate of a pipe, respectively.

This relation can be approximately written as:

$$
T_{t,l}^{S,\text{out}} =
\begin{cases}
T_t^a + \left(T_{l,t}^{S,\text{in}} - T_t^a\right) \cdot \left(1 - \frac{\lambda_l \cdot L_l}{c \dot{m}_{l,t}^{S,\text{pipe}}}\right) & \text{if} \quad \frac{\lambda_l \cdot L_l}{c \dot{m}_{l,t}^{S,\text{pipe}}} \leq 1 \\
T_t^a & \text{if} \quad \frac{\lambda_l \cdot L_l}{c \dot{m}_{l,t}^{S,\text{pipe}}} \geq 1
\end{cases}
\tag{16.23}
$$

$$
T_{t,l}^{R,\text{out}} =
\begin{cases}
T_t^a + \left(T_{l,t}^{S,\text{in}} - T_t^a\right) \cdot \left(1 - \frac{\lambda_l \cdot L_l}{c \dot{m}_{l,t}^{R,\text{pipe}}}\right) & \text{if} \quad \frac{\lambda_l \cdot L_l}{c \dot{m}_{l,t}^{R,\text{pipe}}} \leq 1 \\
T_t^a & \text{if} \quad \frac{\lambda_l \cdot L_l}{c \dot{m}_{l,t}^{R,\text{pipe}}} \geq 1
\end{cases}
\tag{16.24}
$$

Mass Flow Rate Limit

Typically, increasing the flow rate of fluid causes reduction in the ultimate natural frequency of a pipeline. With large velocity of fluid flow, the pipeline can be unstable as the pipeline comes to be exposed to fatigue failure or resonance if its natural frequency is lower than certain limits [25]. Therefore, to avoid pipeline vibrations, the mass flow rates should not surpass their upper boundaries.

$$
\underline{\dot{m}_l^S} \leq \dot{m}_{l,t}^{S,\text{pipe}} \leq \overline{\dot{m}_l^S}
\tag{16.25}
$$

$$
\underline{\dot{m}_l^R} \leq \dot{m}_{l,t}^{R,\text{pipe}} \leq \overline{\dot{m}_l^R}
\tag{16.26}
$$

Pressure Loss

The static pressure drop between two nodes of a pipe is proportionate to the square of mass flow rate. The pressure drop can be stated by (16.27), [24]:

$$
pr_{n+,t}^S - pr_{n-,t}^S = r_l \cdot \left(m_{l,t}^{S,\text{pipe}}\right)^2
\tag{16.27}
$$

$$
pr_{n-,t}^R - pr_{n+,t}^R = r_l \cdot \left(m_{l,t}^{R,\text{pipe}}\right)^2
\tag{16.28}
$$

where r_l is hydraulic resistance of the pipe.

16.3.2.6 Thermal Storage

In this chapter, it is assumed that the hubs with distributed generation are equipped with thermal storages and the heat that the storage unit will be supplied could be presented as following:

$$Es_{h,t} = (1 - \eta_s)\, Es_{h,t-1} + H_{h,t}^{HS} - H_{h,t}^{D} \tag{16.29}$$

The capacity of heat storage is limited as:

$$\underline{Es} \leq Es_{h,t} \leq \overline{Es} \tag{16.30}$$

16.3.3 Load Flow Equations

The electrical power flow constraints in the MCEN scheduling problem are modeled in order to simulate more realistic and precise framework. The flow of power through the power system can be expressed by the following equations which present the active and reactive power flow calculations and characterized by Kirchhoff's laws:

$$P_t^{\text{grid}} + P_{i,t}^g - P_{i,t}^l = \sum_{j=1}^{N_{\text{bus}}} \left(|V_{i,t}| \, |V_{j,t}| \, |Y_{ij}| \cos \left(\theta_{ij,t} - \delta_{i,t} + \delta_{j,t} \right) \right) \tag{16.31}$$

$$Q_t^{\text{grid}} + Q_{i,t}^g - Q_{i,t}^l = -\sum_{j=1}^{N_{\text{bus}}} \left(|V_{i,t}| \, |V_{j,t}| \, |Y_{ij}| \sin \left(\theta_{ij,t} - \delta_{i,t} + \delta_{j,t} \right) \right) \tag{16.32}$$

16.3.3.1 Voltage Limits

The voltage magnitude of substation buses, V_s, should be kept at nominal value V_S^n. Moreover, the bus voltages magnitude, $V_{i,t}$, should be maintained at permissible range.:

$$V_{\min} \leq |V_{i,t}| \leq |V_{\max}| \tag{16.33}$$

$$|V_S| = V_S^n. \tag{16.34}$$

16.3.3.2 Exchangeable Power Limit

In order to have the stable operation, interchangeable apparent power with the main grid should be in its admissible range [26].

$$\sqrt{P_t^{\text{grid}^2} + Q_t^{\text{grid}^2}} \leq \overline{S^{\text{grid}}} \tag{16.35}$$

16.3.3.3 Apparent Power Flow Limits for Branches

It is indispensable to preserve the apparent power flowing from each branch, $S_{br,t}$, of the network in a limited bound:

$$\sqrt{P_{br,t}^2 + Q_{br,t}^2} \leq \overline{S_{br}} \tag{16.36}$$

16.3.4 Demand Response Program

The power and heat generations of hubs are almost correlated as CHP units' heat and power generations are interdependent. The sources of heat provision in the presented model for MCEN are gas furnaces and CHP units and these sources will be feed through bought gas. Hence, despite the constant price of gas, an efficient DRP is essential in MCENs to reduce the total cost. In addition, since the thermal load of a hub can be presumed more responsive and flexible than electrical load, the proposed DRP would be applied to the heat load. It is worth mentioning that, during the scheduling period, the thermal load is assumed to be shiftable and curtailable owing to the thermal load nature. The presented DRP for thermal load can be expressed as following:

$$H_t^{\text{HES}} = \left(1 - \text{cur}_t^{\text{HES}}\right) \times H_t^{\text{HES0}} + sl_t^{\text{HES}} \tag{16.37}$$

$$H_{\text{inc},t}^{\text{HES}} = sl_t^{\text{HES}} - \left(\text{cur}_t^{\text{HES}} \times H_t^{\text{HES0}}\right) \tag{16.38}$$

$$0 \leq H_{\text{inc},t}^{\text{HES}} \leq \text{inc}_t^{\text{HES}} \times H_t^{\text{HES0}} \tag{16.39}$$

$$\text{cur}_t^{\text{HES}} \leq \overline{\text{cur}} \tag{16.40}$$

$$\text{inc}_t^{\text{HES}} \leq \overline{\text{inc}} \tag{16.41}$$

$$H_{\text{Cur}} = \sum_t \sum_{\text{HES}} \left\{ \left(\text{cur}_t^{\text{HES}} \times H_t^{\text{HES0}} \right) - sl_t^{\text{HES}} \right\} \tag{16.42}$$

Equations (16.37) and (16.38) characterize the heat load and incremented heat load after employing the DRP. Equations (16.39), (16.40), and (16.41) restrict the increased load, conveyed load, and percentage of increased load. Equation (16.42) computes the total quantity of curtailed thermal load of MCEN. It should be mentioned that $H_{e,t}^{\text{HES}}$ in the above equations indicates the distribution network exchangers that are assumed as thermal loads.

16.4   Numerical Analysis

To scrutinize the validity and outperformance of the proposed model, a multi-carrier energy system consisting of a district heating and an electrical sub-networks has been employed in this section.

16.4.1   Multi-Carrier Energy System Structure

Figure 16.2 illustrates the structure of this test system. Configuration and characteristics of the multi-carrier energy system units [27] are presented in Tables 16.1 and 16.2, respectively. In the studied MCEN, bus 1 is connected to the main grid and the system is able to procure the electricity from the grid according to the day-ahead market prices. There are three energy hubs in the MCEN and their configurations are accordant with Fig. 16.3. Detailed characteristics of hubs' facilities are provided in Table 16.2. The predicted hourly active and reactive loads for of all buses are depicted in Fig. 16.4. Other network data comprising the impedance of branches are taken from [28]. The minimum and maximum values for voltage magnitude are assumed to be 0.95 p.u. and 1.05 p.u., respectively. Moreover, the gas price is considered 30 \$/MWh [27]. Minimum and maximum limits of hot water supply temperature are 70 °C and 100 °C, respectively. The specific heat of water, C, and the ambient temperature, T_a are 4.182×10^{-3} MJ kg^{-1} °C^{-1} and 10 °C, respectively. Two case studies have been studied to evaluate the proposed model. The first case schedules the MCEN without applying DRP, whereas the second case scrutinizes the impact of heat DRP in the scheduling procedure.
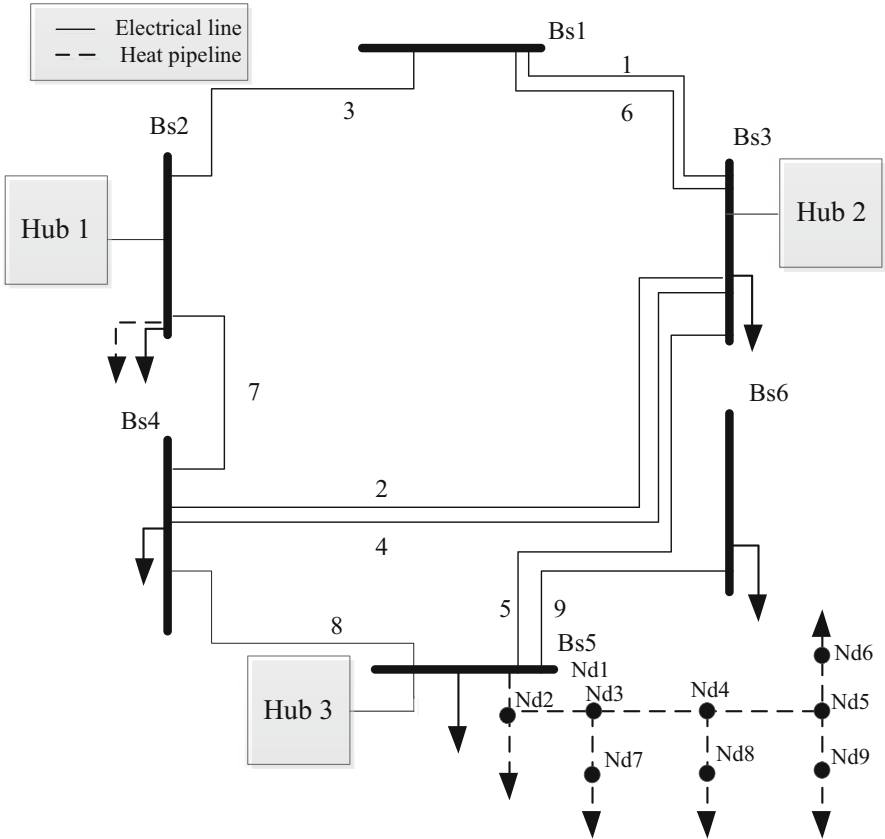
Fig. 16.2 The 3-hub test system under study

Table 16.1 MCEN configuration

Unit\Location	Electrical bus no.	Heat node no.	Hub no.
Generator 1	3	–	2
Gas furnace 1	2	–	1
Gas furnace 2	5	1	3
CHP unit 1	2	–	1
CHP unit 2	5	1	3
Heat storage	2	–	1

Table 16.2 Operational constraints of energy hubs generation units

Device	Efficiency	$\overline{P}$ (kW)	$\underline{P}$ (kW)
Generator of hub 2	$\eta^G = 0.6$	150	0
Gas furnace of hubs 1 & 3	$\eta^F = 0.75$	10	0
CHP units of hubs 1 & 3	$\eta_e^{CHP} = 0.35, \eta_q^{CHP} = 0.45$	100	0
Heat storage of hub 1	$\eta_s = 0.01$	50	0
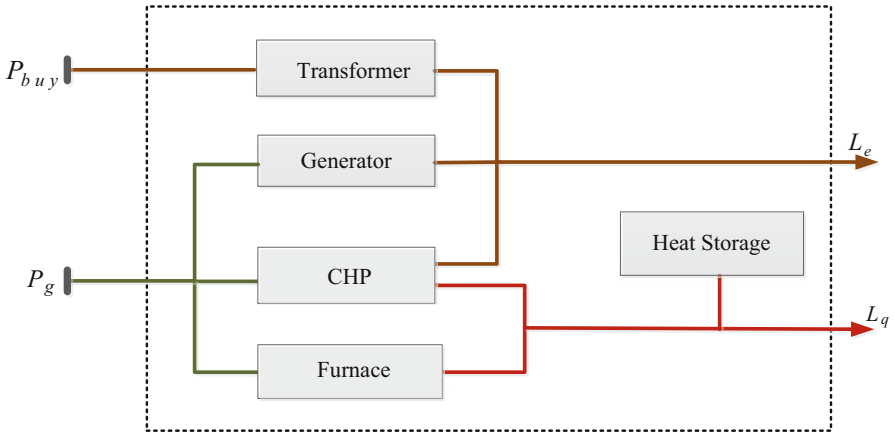
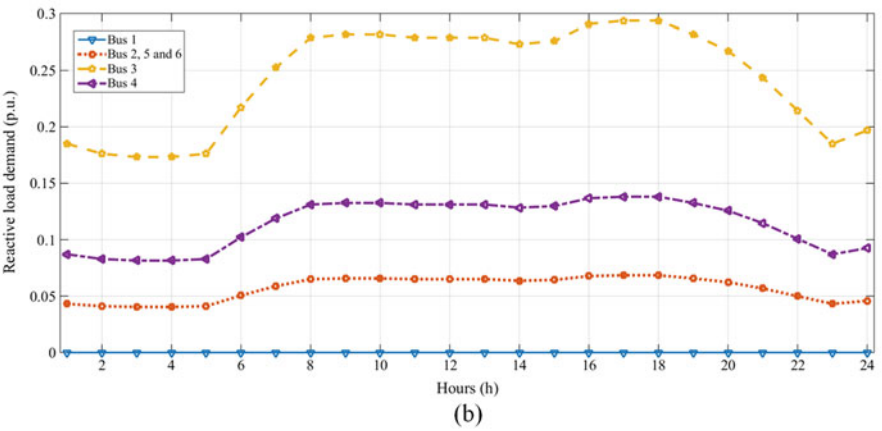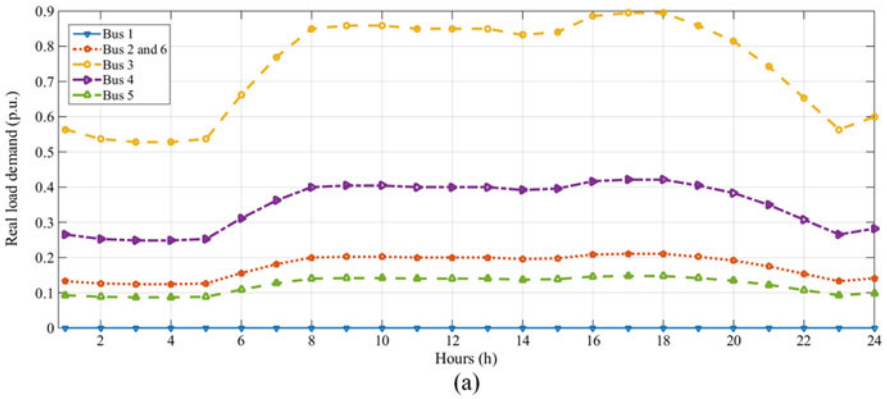**Fig. 16.3** A typical structure of an energy hub

Fig. 16.4 Bus data (**a**) active loads (**b**) reactive loads

16.4.2 Simulation Results

This subsection is developed to study the MCEN scheduling problem employing the proposed framework. The mixed integer non-linear programming (MINLP) model has been applied in GAMS [29] environment unraveled by SBB/CONOPT solver. In the first case, all the economic and technical constraints are taken into account except DRP. Table 16.3 provides the summary of simulation results. Regarding Table 16.3, the cost of MCEN energy providing would be $239.81 for case 1 which has been reduced to $230.225 for the case with DRP. Furthermore, the system revenue from the electricity market participation over 24-hour time interval is about $30.08 for case 1 and $38.264 for case study 2. It can be inferred from the results that implementing DRP in the scheduling process has increased the revenue approximately 27.2% and reduced the total cost about 4%. The voltage magnitude of all buses is presented in Fig. 16.5 for case study 2. Regarding Fig. 16.5, the voltage magnitude of all buses is restricted between 0.95 and 1.05 p.u. Thermal load of DHN and the thermal load with distributed generation are depicted in Fig. 16.6. Fig. 16.7 shows the supply temperature of node 1 in DHN. According to Fig. 16.7, the temperature is decreased when the thermal demand is low in order to diminish losses. Moreover, the temperature is enhanced once the thermal demand is incremented to decrease the power expended by the pump. However, the temperature is reduced in some intervals that the thermal demand is high. This fact is due to the interdependency of heat and power generations of CHP facilities and the

Table 16.3 Summarized simulation results of MCEN

	Generation cost	Revenue from the sale of power	Cost of buying power	Value of objective function
Case study 1	$221.471	$30.081	$48.420	$239.810
Case study 2	$217.198	$38.264	$51.291	$230.225
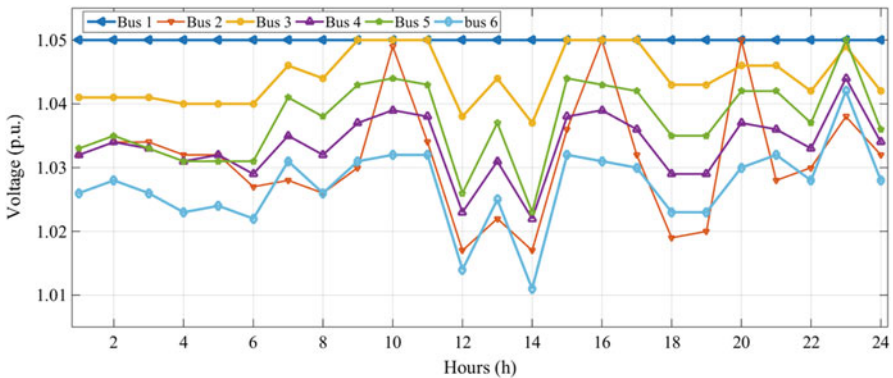
Fig. 16.5 Voltage profile of some electrical buses during 24 h
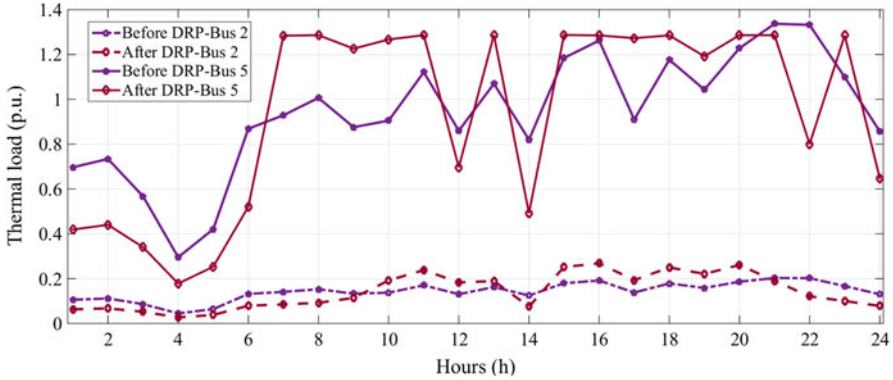
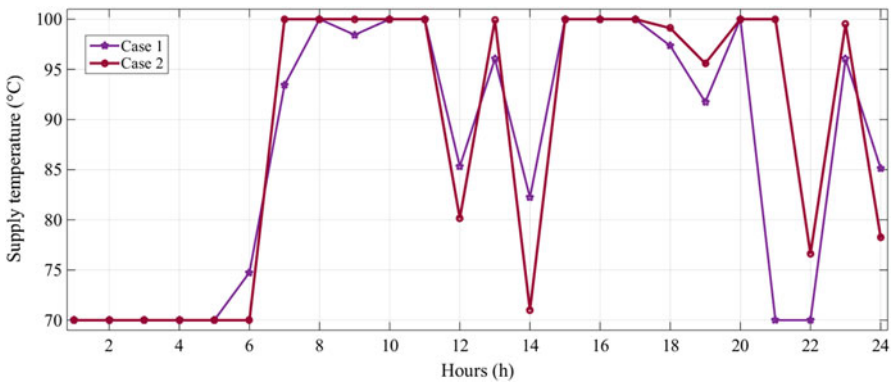**Fig. 16.6** Hourly heat demand of the hubs

Fig. 16.7 Supply temperature of node 1

active power demand of power network. It is worth mentioning that the temperature in hours 21 and 22 has been improved by applying DRP. According to the simulation results, the temperature has been increased in these hours to decrease the consumed power by the pump.

Figure 16.8 depicts the gas distribution among DHN and hub 2's converters for case 1. Referring to this figure, it could be perceived that the gas furnace of DHN will contribute in providing thermal energy only when the CHP unit's capacity is reached, i.e. in hours 21:00 and 22:00. In addition, the CHP unit 1 is the only supplier of hub 1. According to the simulation results, the heat storage would be discharged till hour 24:00 to reduce the total cost. In addition, gas furnaces will not participate in providing thermal energy after applying DRP. The simulations indicate the similar results for case 2, except that by applying the DRP, the heat demand profile will be modified in a way that there will be no need to gas furnaces.
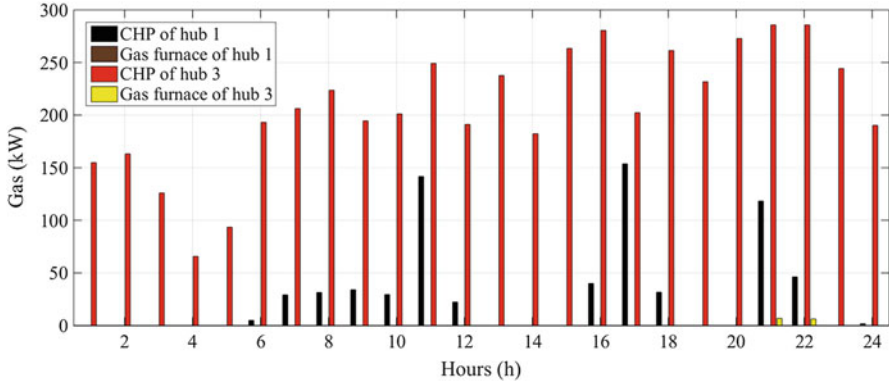
Fig. 16.8 Gas distribution among the hubs converters for case 1

16.5 Conclusion

In recent days, energy systems' optimal operation is a fundamental issue in system management scrutiny. This chapter has proposed a model for optimal scheduling of MCENs consisting of district heating and electrical networks. In the presented energy hub framework, the energy and continuity laws as well as the characteristic of district heating system's major elements for DHN, voltage magnitude of buses and line flow limits of electric network are modeled successfully. In addition, since the heating load profile of the MCEN can be modified, heat DRP has been implemented in order to handle the interdependency of heat and power in CHP units. The simulation outcomes have verified the usefulness and efficiency of the entire MCEN model and the capability of DRP, which can be employed to optimize the model. According to the simulation results, applying the heat DRP to the DHN reduces the total cost about 4% in the studied case. The results also indicate that the optimal operating strategy can improve the optimal temperature of nodes and decrease the consumed power by the pump.

Nomenclature

Indices

h	Index of hubs.
n	Index of nodes in the heating network.
l	Indices of pipelines in the heating network.
s	Superscript of supply in the heating network.
R	Superscript of return in the heating network.

n^+ Index of starting node of pipeline l.
n^- Index of ending node of pipeline l.
i Index of buses in the electricity network.

Variables

H_t^{HS} Total heat output of hub h.
T Temperature in the heating network.
pr Pressure in the heating network.
$P_{i,t}^g$ Active power flow of hubs positioned on bus i.
$Q_{i,t}^g$ Reactive power flow of hubs positioned on bus i.
$V_{i,t}$ Voltage of bus i.
$Pg_{h,t}$ Pumping power.
P_t^{grid} Active power bought from the Utility.
Q_t^{grid} Reactive power bought from the Utility.
$P_{h,t}^{pump}$ Pumping power.
$\dot{m}$ Mass flow rate.
cur_t^{HES} The participation factor of load in DRP.
sl_t^{HES} The amount of transferred load from other hours to hour t.
inc_t^{HES} Incremental load factor.
H_{Cur} Total quantity of curtailed heat load.
$H_{inc,t}^{HES}$ The increased load.
H_t^{HS} Total heat output of hub h.
T Temperature in the heating network.

Parameters

N_{bus} Number of buses of the power system.
H_t^{HES0} The primitive hub's load.
$P_{i,t}^l$ Active load of bus i.
$Q_{i,t}^l$ Reactive load of bus i.
Y_{ij} Magnitude of feeder's admittance.
$\theta_{ij,t}$ Phase angle of feeder's admittance.
$\gamma_{g,t}$ Gas price.
$\gamma_{e,t}$ Predicted day-ahead electricity market price.
η Efficiency.
N_{bus} Number of buses of the power system.
H_t^{HES0} The primitive hub's load.
$P_{i,t}^l$ Active load of bus i.

References

1. Gebremedhin A (2014) Optimal utilisation of heat demand in district heating system—a case study. Renew Sust Energ Rev 30:230–236
2. Geidl M, Andersson G (2007) Optimal power flow of multiple energy carriers. IEEE Trans Power Syst 22(1):145–155
3. Flexible energy delivery systems. http://www.cardiff.ac.uk/ugc/flexibleenergy-delivery-system-seminar-series-for-postgraduates-and-researchers. Accessed 25 Mar 13
4. Moeini-Aghtaie M, Abbaspour A, Fotuhi-Firuzabad M, Hajipour E (2014) A decomposed solution to multiple-energy carriers optimal power flow. IEEE Trans Power Syst 29(2):707–716
5. Geidl M, Andersson G (2006) Operational and structural optimization of multi-carrier energy systems. Eur T Electr Power 16(5):463–477
6. Barbieri ES et al (2014) Optimal sizing of a multi-source energy plant for power heat and cooling generation. Appl Therm Eng 71(2):736–750
7. Geidl M, Koeppel G, Favre-Perrod P, Klockl B, Andersson G, Frohlich K (2007) Energy hubs for the future. IEEE Power Energ Mag 5(1):24–30
8. Salimi M, Ghasemi H, Adelpour M, Vaez-ZAdeh S (2015) Optimal planning of energy hubs in interconnected energy systems: a case study for natural gas and electricity. IET Gener Transm Distrib 9(8):695–707
9. Anders GJ, Vaccaro A (2011) Innovations in power systems reliability. Springer, London
10. Krause T, Andersson G, Frohlich K, Vaccaro A (2011) Multiple-energy carriers: modeling of production, delivery, and consumption. Proc IEEE 99(1):15–27
11. Alipour M, Zare K, Mohammadi-Ivatloo B (2016) Optimal risk-constrained participation of industrial cogeneration systems in the day-ahead energy markets. Renew Sust Energ Rev 60:421–432
12. Parisio A, Del Vecchio C, Vaccaro A (2012) A robust optimization approach to energy hub management. Int J Electr Power Energy Syst 42(1):98–104
13. Martinez-Mares A, Fuerte-Esquivel CR (2012) A unified gas and power flow analysis in natural gas and electricity coupled networks. IEEE Trans Power Syst 27(4):2156–2166
14. Shabanpour-Haghighi A, Seifi AR (2015) Energy flow optimization in multicarrier systems. IEEE Trans Ind Inf 11(5):1067–1077
15. Medina J, Muller N, Roytelman I (2010) Demand response and distribution grid operations: opportunities and challenges. IEEE Trans Smart Grid 1(2):193–198
16. Mathieu JL, Price PN, Kiliccote S, Piette MA (2011) Quantifying changes in building electricity use, with application to demand response. IEEE Trans Smart Grid 2(3):507–518
17. Wu H, Shahidehpour M, Al-Abdulwahab A (2013) Hourly demand response in day-ahead scheduling for managing the variability of renewable energy. IET Gener Transm Distrib 7(3):226–234
18. Mosaddegh A, Canizares CA, Bhattacharya K (2017) Optimal demand response for distribution feeders with existing smart loads. IEEE Trans Smart Grid:1
19. Pazouki S, Haghifam MR, Olamaei J (2013) Economical scheduling of multi carrier energy systems integrating renewable, energy storage and demand response under energy hub approach. In: Smart Grid Conference (SGC), IEEE, pp 80–84
20. Bahrami S, Sheikhi A (2016) From demand response in smart grid toward integrated demand response in smart energy hub. IEEE Trans Smart Grid 7(2):650–658
21. Garage G Human comfort zone. [Online]. http://www.greengaragedetroit.com/index.php?title=HumanComfortZone
22. Liu X, Wu J, Jenkins N, Bagdanavicius A (2016) Combined analysis of electricity and heat networks. Appl Energy 162:1238–1250
23. Zhao H (1995) Analysis, modelling and operational optimization of district heating systems. PhD Thesis, Technical University of Denmark

24. Awad B, Chaudry M, Wu J, Jenkins N (2009) Integrated optimal power flow for electric power and heat in a microgrid. In: 20th international conference and exhibition on electricity distribution-part 1, 2009. CIRED 2009, IET, pp 1–4

25. Grant I (2010) Flow induced vibrations in pipes, a finite element approach. M.S. thesis, Department of Mechanical Engineering, Cleveland State University, Cleveland, OH, USA

26. Aghaei J, Alizadeh MI (2013) Multi-objective self-scheduling of CHP (combined heat and power)-based microgrids considering demand response programs and ESSs (energy storage systems). Energy 55:1044–1054

27. Alipour M, Zare K, Abapour M (2017) MINLP probabilistic scheduling model for demand response programs integrated energy hubs. IEEE Trans Ind Inf 14:79. https://doi.org/10.1109/TII.2017.2730440

28. Alipour M, Zare K, Seyedi H (2017) Power flow constrained short-term scheduling of CHP units. In: Sustainable development in energy systems. Springer, Cham, pp 147–165

29. Brooke AD, Kendrick AM, Roman R (1998) GAMS: a user's guide. GAMS Development, Washington, DC